An assessment of a higher order theory for composite laminates subjected to thermal gradient

Tarun Kant [a], S.M. Shiyekar [b,*]

[a] Department of Civil Engineering, Indian Institute of Technology Bombay, Powai, Mumbai 400 076, India
[b] Department of Civil Engineering, Rajaramnagar (Sakhrale), Islampur, Walva, Sangli, Maharashtra 415 414, India

ARTICLE INFO

ABSTRACT

A complete analytical model, which incorporates shear deformation as well as transverse normal thermal strains is assessed for the thermal stress analysis of cross-ply laminates subjected to linear or gradient thermal profile across thickness of the laminate. Primary displacement field is expanded in the thickness direction using twelve degrees of freedom. Equilibrium equations in the present higher order shear and normal deformation theory (HOSNT12) are variationally consistent and obtained using principle of virtual work [1]. Numerical results of displacements and stresses are compared with three dimensional (3D) elasticity solution and other two dimensional (2D) models.

© 2012 Elsevier Ltd. All rights reserved.

1. Introduction

Multilayered composites have found wide use in many weight-sensitive structures such as aircraft and missile structural components, where high strength-to-weight and stiffness to-weight ratios are essentials. A laminate is a multilayered composite made up of several individual elastic layers called laminae. Every laminae consists of fibers oriented in a specific direction to provide efficiently the required strength and stiffness to laminate. Thermal stress analysis is important in composite laminates due to high transverse stresses and different thermal expansion coefficients in the orthotropic layers of laminate. Delamination of layers and longitudinal cracks in the matrix are the few failure modes in the laminate because of severe thermal loading and requires accurate prediction of interlaminar stresses. Higher order shear and normal deformation theory (HOSNT12) is used to find thermally induced stresses in the composite laminates. Normal deformation plays very important role in the thermal analysis because of high thermal expansion coefficient in the thickness direction.

Thermal stress analysis of isotropic beams, plates and shells using classical laminated plate theory (CLPT) can be accessible from Timoshenko and Woinowsky-Krieger [2]. Most of the early research which is based on first order shear deformation theory (FOST) [3,4], which included the thermal effects on laminates were Reddy and Chao [5] developed finite element (FE) formulation of laminates subjected to thermal loading based on FOST. Argyris and Tenek [6] used linear thermal variation across the thickness of the laminates to formulate FE model based on the first order shear deformation theory. The prime objective of HOST models is to remove the deficiencies from the CLPT and FOST. Cubic variation is assumed in the in-plane displacement field resulting in parabolic variation in the transverse shear stress with no need to consider shear correction factors. Khdeir and Reddy [7] developed refined plate theories to study the thermal stresses and deformations of cross-ply rectangular laminates using stress-space approach. Kant and Khare [8] developed a simple C° iso-parametric finite element (FE) displacement model based on HOST formulations for the analysis of symmetric and unsymmetric laminates subjected to thermal gradient. Rohwer et al. [9] removed the deficiencies in the FOST by incorporating third and fifth order displacement approximations through the plate thickness. 3D elasticity equations can estimate the correct results of the thermally induced quantities like displacements and stresses. Tungikar and Rao [10] obtained 3D elasticity solution for temperature distribution and thermal stresses in simply supported rectangular laminates. The actual temperature distribution across the thickness of the laminate is evaluated by solving the ordinary differential equations (ODEs) of heat conduction without internal heat generation. The actual profile also satisfies the interface heat flux continuity. Savoia and Reddy [11] also solved transient heat conduction equation for exact temperature distribution across the thickness of laminates for 3D stress analysis of symmetric four-layered square laminate subjected to sudden uniform temperature change. Bhaskar et al. [12] developed 3D elasticity solution for laminates under cylindrical and bi-directional bending by assuming linear variation of thermal profile through the thickness of the symmetric laminate. Kapuria and Achary [13] assessed higher order zig-zag (HZIGT) model along

* Corresponding author. Tel.: +91 98223 77577; fax: +91 2342 220989.
 E-mail address: sandeep.shiyekar@ritindia.edu (S.M. Shiyekar).

with exact, zig-zag (ZIGT) and third order theory (TOT) models for composite laminates subjected various thermal profiles across the thickness. Kant et al. [14] developed semi-analytical solution for constant and linear temperature variation through the thickness of a laminated composites and sandwiches.

Here, in this paper we assess various approximate theories in view of 3D exact solutions for laminates subjected to thermal loading.

2. Higher order formulation

A complete analytical formulation and solution for a laminate simply (diaphragm) supported on all the sides is presented. The geometry of the laminate is such that the side 'a' is along 'x' axis and side 'b' is on 'y' axis. The thickness of the laminate is denoted by 'h' and is coinciding with 'z' axis. The reference mid-plane of the laminate is at $h/2$ from top or bottom surface of the laminate as shown in Fig. 1. The lamina reference axes system is also shown in the figure with fiber direction. Figure also illustrates the mid-plane positive set of displacements along (x–y–z) axes.

From linear theory of elasticity, the general strain–displacement relationships for small displacements can be stated as under.

$$
\begin{Bmatrix} \varepsilon_x \\ \varepsilon_y \\ \varepsilon_z \\ \gamma_{xy} \\ \gamma_{yz} \\ \gamma_{xz} \end{Bmatrix} = \left\{ \frac{\partial u}{\partial x}, \; \frac{\partial v}{\partial y}, \; \frac{\partial w}{\partial z}, \; \frac{\partial u}{\partial y}+\frac{\partial v}{\partial x}, \; \frac{\partial v}{\partial z}+\frac{\partial w}{\partial y}, \; \frac{\partial u}{\partial z}+\frac{\partial w}{\partial x} \right\}^t \tag{1}
$$

Principal material coordinate system (1–2–3) is used for the stress–strain relationship of fiber-reinforced composites. The axis 1 is aligned with the fiber direction, the axis 2 is perpendicular to the fibers but in the plane of the layer, and axis 3 is perpendicular to the fibers as well as to the plane of layer. The stress–strain–temperature relationship in 1–2–3 coordinate system can be written as [15].

$$
\begin{aligned}
\varepsilon_1 &= \frac{\sigma_1}{E_1} - v_{21}\frac{\sigma_2}{E_2} - v_{31}\frac{\sigma_3}{E_3} + \alpha_1 T, \\
\varepsilon_2 &= -v_{12}\frac{\sigma_1}{E_1} + \frac{\sigma_2}{E_2} - v_{32}\frac{\sigma_3}{E_3} + \alpha_2 T, \\
\varepsilon_3 &= -v_{13}\frac{\sigma_1}{E_1} - v_{23}\frac{\sigma_2}{E_2} + \frac{\sigma_3}{E_3} + \alpha_3 T, \\
\gamma_{12} &= \frac{\tau_{12}}{G_{12}}, \gamma_{23} = \frac{\tau_{23}}{G_{23}}, \gamma_{13} = \frac{\tau_{13}}{G_{13}}
\end{aligned} \tag{2}
$$

The above relationship for Lth orthotropic elastic layer can be written in a matrix form as:

$$
\begin{Bmatrix} \varepsilon_1 \\ \varepsilon_2 \\ \varepsilon_3 \\ \gamma_{12} \\ \gamma_{23} \\ \gamma_{13} \end{Bmatrix}^L = \begin{bmatrix} \frac{1}{E_1} & \frac{-v_{21}}{E_2} & \frac{-v_{31}}{E_3} & 0 & 0 & 0 \\ \frac{-v_{12}}{E_1} & \frac{1}{E_2} & \frac{-v_{32}}{E_3} & 0 & 0 & 0 \\ \frac{-v_{13}}{E_1} & \frac{-v_{23}}{E_2} & \frac{1}{E_3} & 0 & 0 & 0 \\ 0 & 0 & 0 & \frac{1}{G_{12}} & 0 & 0 \\ 0 & 0 & 0 & 0 & \frac{1}{G_{23}} & 0 \\ 0 & 0 & 0 & 0 & 0 & \frac{1}{G_{13}} \end{bmatrix}^L \begin{Bmatrix} \sigma_1 \\ \sigma_2 \\ \sigma_3 \\ \tau_{12} \\ \tau_{23} \\ \tau_{13} \end{Bmatrix}^L + \begin{Bmatrix} \alpha_1 T \\ \alpha_2 T \\ \alpha_3 T \\ 0 \\ 0 \\ 0 \end{Bmatrix}^L \tag{3}
$$

It also can be written in a compact form as: $\{\varepsilon_i\}^L = [S_{ij}]^L\{\sigma_i\}^L + \{\alpha_i\}T$ where, $[S_{ij}]$ associated with this relationship is known as compliance matrix and the inverse of the compliance matrix is stiffness matrix or elasticity matrix $[C_{ij}]$.

As stated in Eq. (3), the compliance matrix involves 12 engineering properties: three extensional moduli (E_1, E_2, E_3), six Poisson's ratios (v_{12}, v_{21}, v_{23}, v_{32}, v_{13}, v_{31}) and three shear moduli
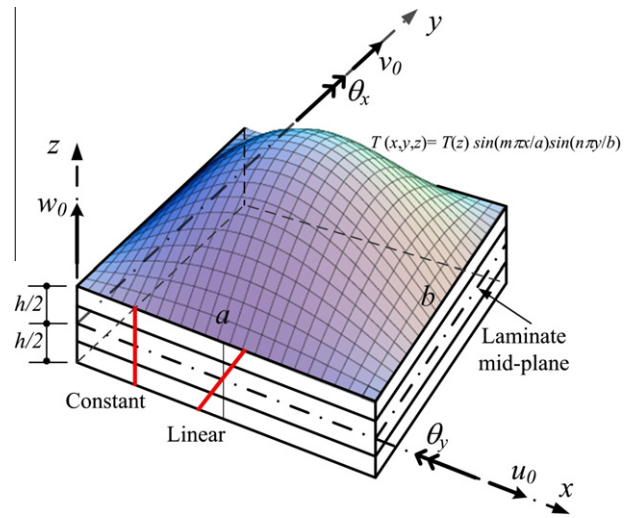
Fig. 1. Laminate geometry with positive set of lamina/laminate reference axes, positive displacement components, fiber orientation and thermal loading across the thickness of the laminate.

(G_{12}, G_{23}, G_{13}). These 12 engineering properties are not independent. Since compliance matrix is symmetric, there are only nine independent elastic properties with following relationships.

$$
\frac{v_{21}}{E_2} = \frac{v_{12}}{E_1}, \quad \frac{v_{31}}{E_3} = \frac{v_{13}}{E_1}, \quad \frac{v_{32}}{E_3} = \frac{v_{23}}{E_2}. \tag{4}
$$

The 3D stress–strain constitutive relationship with stiffness matrix $[C_{ij}]$ for Lth lamina w.r.t. 1–2–3 coordinate system can be written as:

$$
\begin{Bmatrix} \sigma_1 \\ \sigma_2 \\ \sigma_3 \\ \tau_{12} \\ \tau_{23} \\ \tau_{13} \end{Bmatrix}^L = \begin{bmatrix} C_{11} & C_{12} & C_{13} & 0 & 0 & 0 \\ C_{12} & C_{22} & C_{23} & 0 & 0 & 0 \\ C_{13} & C_{23} & C_{33} & 0 & 0 & 0 \\ 0 & 0 & 0 & C_{44} & 0 & 0 \\ 0 & 0 & 0 & 0 & C_{55} & 0 \\ 0 & 0 & 0 & 0 & 0 & C_{66} \end{bmatrix}^L \begin{Bmatrix} \varepsilon_1 - \alpha_1 T \\ \varepsilon_2 - \alpha_2 T \\ \varepsilon_3 - \alpha_3 T \\ \gamma_{12} \\ \gamma_{23} \\ \gamma_{13} \end{Bmatrix}^L \tag{5}
$$

in which,

$$
C_{11} = \frac{E_1(1 - v_{23}v_{32})}{\Delta}; \quad C_{12} = \frac{E_1(v_{21} + v_{31}v_{23})}{\Delta};
$$
$$
C_{13} = \frac{E_1(v_{31} + v_{21}v_{32})}{\Delta};
$$

$$
C_{22} = \frac{E_2(1 - v_{13}v_{31})}{\Delta}; \quad C_{23} = \frac{E_2(v_{32} + v_{12}v_{31})}{\Delta};
$$
$$
C_{33} = \frac{E_3(1 - v_{12}v_{21})}{\Delta};
$$

$$
C_{44} = G_{12}; \quad C_{55} = G_{23}; \quad C_{66} = G_{13}. \tag{6}
$$

and $\Delta = (1 - v_{12}v_{21} - v_{23}v_{32} - v_{31}v_{13} - 2v_{12}v_{23}v_{31})$.

In the laminate coordinate system (x–y–z) the stress strain relationship for Lth lamina can be written as

$$
\begin{Bmatrix} \sigma_x \\ \sigma_y \\ \sigma_z \\ \tau_{xy} \\ \tau_{yz} \\ \tau_{xz} \end{Bmatrix}^L = \begin{bmatrix} Q_{11} & Q_{12} & Q_{13} & Q_{14} & 0 & 0 \\ Q_{12} & Q_{22} & Q_{23} & Q_{24} & 0 & 0 \\ Q_{13} & Q_{23} & Q_{33} & Q_{34} & 0 & 0 \\ Q_{14} & Q_{24} & Q_{34} & Q_{44} & 0 & 0 \\ 0 & 0 & 0 & 0 & Q_{55} & Q_{56} \\ 0 & 0 & 0 & 0 & Q_{56} & Q_{66} \end{bmatrix}^L \begin{Bmatrix} \varepsilon_x - \alpha_x T \\ \varepsilon_y - \alpha_y T \\ \varepsilon_z - \alpha_z T \\ \gamma_{xy} \\ \gamma_{yz} \\ \gamma_{xz} \end{Bmatrix}^L \tag{7}
$$

where (σ_x, σ_y, σ_z, τ_{xy}, τ_{yz}, τ_{xz}) are the stresses and (ε_x, ε_y, ε_z, γ_{xy}, γ_{yz}, γ_{xz}) are the strains with respect to laminate coordinate

Table 1
Elastic and thermal material properties.

Example	Reference	Properties	Normalization
2	[12]	$E_L/E_T = 25$, $G_{LT}/E_T = 0.5$, $G_{TT}/E_T = 0.2$, $v_{LT} = v_{TT} = 0.25$, $\alpha_T/\alpha_L = 1125$.	$\bar{w} = \dfrac{w}{h\alpha_L T_0 S^2}$, $(\bar{u}, \bar{v}) = \dfrac{(u, v)}{h\alpha_L T_0 S}$, $(\bar{\sigma}_i, \bar{\tau}_{ij}) = \dfrac{(\sigma_i, \tau_{ij})}{E_T \alpha_L T_0}$.
1, 2	[16]	$E_L/E_T = 15, E_T = 10$ GPa, $G_{LT}/E_T = 0.3356$, $v_{LT} = 0.3$, $v_{TT} = 0.3$, $\alpha_L/\alpha_0 = 0.015$, $\alpha_T/\alpha_0 = 1.0$.	$(\bar{u}, \bar{v}, \bar{w}) = \dfrac{(u, v, w)}{\alpha_0 T_0 h}$, $(\bar{\sigma}_i, \bar{\tau}_{ij}) = \dfrac{(\sigma_i, \tau_{ij})}{\alpha_0 T_0 E_0}$. $\alpha_0 = 10^{-6}/K, E_0 = 1$ GPa
3, 4, 5	[13]	$E_L = 181,\ E_T = 10.3$ GPa, $G_{LT} = 7.17$ GPa, $G_{TT} = 2.87$ GPa $v_{LT} = 0.28$, $v_{TT} = 0.33$, $\alpha_L = 0.02 \times 10^{-6}$ K^{-1}, $\alpha_T = 22.5 \times 10^{-6}$ K^{-1}. $\lambda_L = 1.5\ W_m^{-1}\ K^{-1}$, $\lambda_T = 0.5\ W_m^{-1}\ K^{-1}$	$(\bar{u}, \bar{v}, \bar{w}) = \dfrac{100(u, v, w/S)}{\alpha_T S h T_0}$, $(\bar{\sigma}_x, \bar{\sigma}_y) = \dfrac{(\sigma_x, \sigma_y)}{\alpha_T E_T T_0}$, $(\bar{\tau}_{yz}, \bar{\tau}_{xz}, \bar{\sigma}_z) = \dfrac{(\tau_{yz}, \tau_{xz}, S\sigma_z)S}{\alpha_T E_T T_0}$.

system (x–y–z). [Q_{ij}] are transformed elastic constants or stiffness matrix and defined as per the following.

$$Q_{11} = C_{11}c^4 + 2(C_{12} + 2C_{44})s^2c^2 + C_{22}s^4; \quad Q_{12} = C_{12}(c^4 + s^4) + (C_{11} + C_{22} - 4C_{44})s^2c^2;$$
$$Q_{13} = C_{13}c^2 + C_{23}s^2; \quad Q_{14} = (C_{11} - C_{12} - 2C_{44})sc^3 + (C_{12} - C_{22} + 2C_{44})cs^3;$$
$$Q_{22} = C_{11}s^4 + C_{22}c^4 + (2C_{12} + 4C_{44})s^2c^2; \quad Q_{23} = C_{13}s^2 + C_{23}c^2;$$
$$Q_{24} = (C_{11} - C_{12} - 2C_{44})s^3c + (C_{12} - C_{22} + 2C_{44})c^3s; \quad Q_{33} = C_{33};$$
$$Q_{34} = (C_{31} - C_{32})sc; \quad Q_{44} = (C_{11} - 2C_{12} + C_{22} - 2C_{44})c^2s^2 + C_{44}(c^4 + s^4);$$
$$Q_{55} = C_{55}c^2 + C_{66}s^2; \quad Q_{56} = (C_{66} - C_{55})cs; \quad Q_{66} = C_{55}s^2 + C_{66}c^2$$

$$(8)$$

and $Q_{ij} = Q_{ji}$, $i, j = 1$–6, where, $c = \cos(\alpha)$ and $s = \sin(\alpha)$, α is the angle made by fiber direction to x-axis. The transformations of coefficients of linear thermal expansion are given by

$$\alpha_x = \alpha_1 c^2 + \alpha_2 s^2; \quad \alpha_y = \alpha_1 s^2 + \alpha_2 c^2; \quad \alpha_z = \alpha_3 \quad (9)$$

where α_1, α_2, α_3 are the linear thermal expansion coefficients with respect to lamina reference axes and α_x, α_y, α_z are the linear thermal expansion coefficients with respect to laminate reference axes. T is rise in temperature with respect to reference temperature. The expansion effects are linearly proportional to the temperature change. The free thermal strains do not have any shearing deformations with respect to lamina reference axes.

2.1. Displacement field

In order to approximate the 3D elasticity problem to a 2D plate problem, the displacement components $u(x, y, z)$, $v(x, y, z)$ and $w(x, y, z)$ at any point in the plate space are expanded in a Taylor series in terms of thickness coordinate z, viz.,

$$u(x, y, z) = u(x, y, 0) + z\left(\frac{\partial u}{\partial z}\right)_0 + \frac{1}{2!}z^2\left(\frac{\partial^2 u}{\partial z^2}\right)_0 + \frac{1}{3!}z^3\left(\frac{\partial^3 u}{\partial z^3}\right)_0 + \ldots + \infty$$

$$v(x, y, z) = v(x, y, 0) + z\left(\frac{\partial v}{\partial z}\right)_0 + \frac{1}{2!}z^2\left(\frac{\partial^2 v}{\partial z^2}\right)_0 + \frac{1}{3!}z^3\left(\frac{\partial^3 v}{\partial z^3}\right)_0 + \ldots + \infty$$

$$w(x, y, z) = w(x, y, 0) + z\left(\frac{\partial w}{\partial z}\right)_0 + \frac{1}{2!}z^2\left(\frac{\partial^2 w}{\partial z^2}\right)_0 + \frac{1}{3!}z^3\left(\frac{\partial^3 w}{\partial z^3}\right)_0 + \ldots + \infty$$

$$(10)$$

The first four terms of in-plane displacements (u, and v) involve a nonlinear (cubic) variation through the thickness of the plate and thus the warping of the transverse cross section is integrated in the displacement field. The linear, quadratic and cubic terms in the transverse displacement (w) gives rise to non-zero transverse normal strain and stress. Thus the limitations of CPT as well as FOST are finally eliminated.

Displacement field given by Eq. (10) is written in a concise form and named HOSNT12 [1], as:

$$u(x, y, z) = u_0(x, y) + z\theta_x(x, y) + z^2 u_0^*(x, y) + z^3 \theta_x^*(x, y)$$
$$v(x, y, z) = v_0(x, y) + z\theta_y(x, y) + z^2 v_0^*(x, y) + z^3 \theta_y^*(x, y) \quad (11)$$
$$w(x, y, z) = w_0(x, y) + z\theta_z(x, y) + z^2 w_0^*(x, y) + z^3 \theta_z^*(x, y)$$

The parameter u_0, v_0 are the in-plane displacement and w_0 is the transverse displacement of the middle plane. The θ_x, θ_y are the rotation of the normal to the middle-plane about y and x–axes respectively. The other parameters $u_0^*, v_0^*, w_0^*, \theta_x^*, \theta_y^*, \theta_z^*$ are the corresponding higher order terms in the Taylor's series expansion defined at mid-plane.
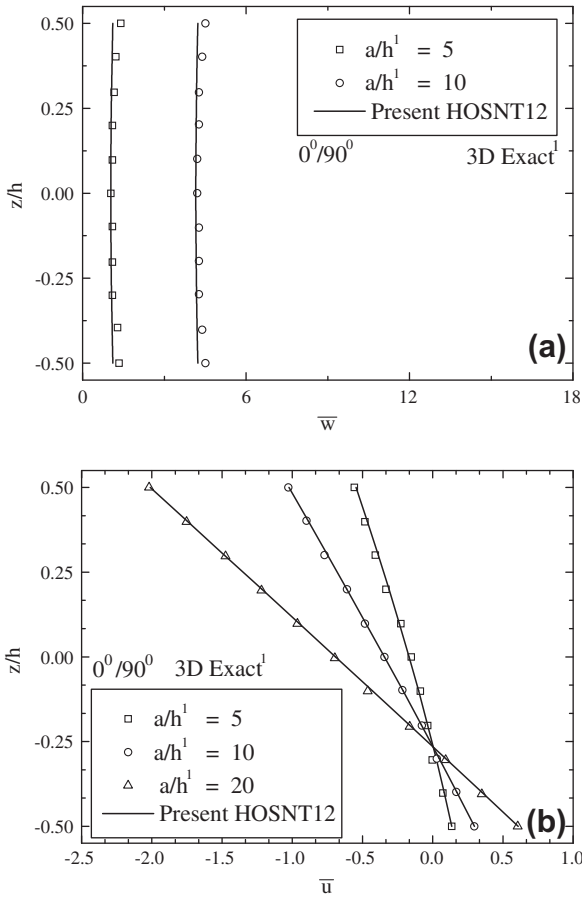
Fig. 2. Variation of normalized (a) transverse displacement $\bar{w}$, and (b) inplane displacement $\bar{u}$ through the thickness of a unsymmetric [0°/90°] laminate under gradient thermal loading for a/h = 5, 10, and 20.
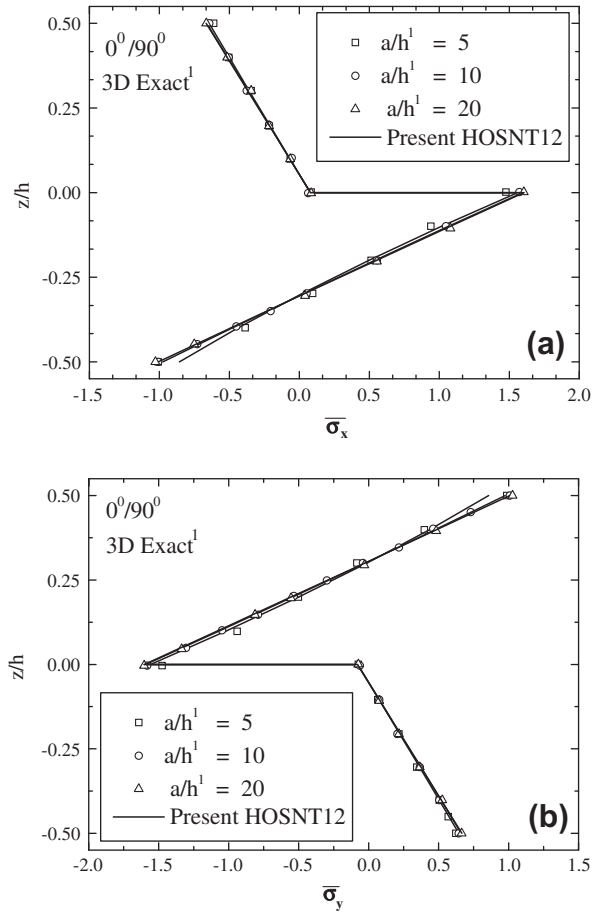
Fig. 3. Variation of normalized in-plane normal stress (a) $\bar{\sigma}_x$, and (b) $\bar{\sigma}_y$ through the thickness of an unsymmetric [0°/90°] laminate under gradient thermal loading for a/h = 5, 10, and 20.

2.2. Governing equations of equilibrium

The principle of minimum potential energy is used, i.e.,

$$\delta(U + V) = 0 \tag{12}$$

where U is the total strain energy due to deformation, V is the potential of the external loads and $U + V = \pi$ is the total potential energy. δ is the variational symbol. Substituting the appropriate energy expression in the above equation, the final expression is written as:

$$\left[\int_{-h/2}^{+h/2}\int_A (\sigma_x\delta\varepsilon_x + \sigma_y\delta\varepsilon_y + \sigma_z\delta\varepsilon_z + \tau_{xy}\delta\gamma_{xy} + \tau_{yz}\delta\gamma_{yz} + \tau_{xz}\delta\gamma_{xz})dAdz \right.$$
$$\left. - \int_A q_z^+ \delta w^+ dA\right] = 0 \tag{13}$$

The following equations of equilibrium are obtained

$$\delta u_0 : \frac{\partial N_x}{\partial x} + \frac{\partial N_{xy}}{\partial y} = 0, \quad \delta v_0 : \frac{\partial N_y}{\partial y} + \frac{\partial N_{xy}}{\partial x} = 0, \quad \delta w_0 : \frac{\partial Q_x}{\partial x} + \frac{\partial Q_y}{\partial y} + (q_z^+) = 0$$

$$\delta\theta_x : \frac{\partial M_x}{\partial x} + \frac{\partial M_{xy}}{\partial y} - Q_x = 0, \quad \delta\theta_y : \frac{\partial M_y}{\partial y} + \frac{\partial M_{xy}}{\partial x} - Q_y = 0$$

$$\delta\theta_z : \frac{\partial S_x}{\partial x} + \frac{\partial S_y}{\partial y} - N_z + \frac{h}{2}(q_z^+) = 0$$

$$\tag{14}$$

$$\delta u_0^* : \frac{\partial N_x^*}{\partial x} + \frac{\partial N_{xy}^*}{\partial y} - 2S_x = 0, \quad \delta v_0^* : \frac{\partial N_y^*}{\partial y} + \frac{\partial N_{xy}^*}{\partial x} - 2S_y = 0$$

$$\delta w_0^* : \frac{\partial Q_x^*}{\partial x} + \frac{\partial Q_y^*}{\partial y} - 2M_z + \frac{h^2}{4}(q_z^+) = 0, \quad \delta\theta_x^* : \frac{\partial M_x^*}{\partial x} + \frac{\partial M_{xy}^*}{\partial y} - 3Q_x^*$$
$$= 0$$

$$\delta\theta_y^* : \frac{\partial M_y^*}{\partial y} + \frac{\partial M_{xy}^*}{\partial x} - 3Q_y^* = 0, \quad \delta\theta_z^* : \frac{\partial S_x^*}{\partial x} + \frac{\partial S_y^*}{\partial y} - 3N_z^* + \frac{h^3}{8}(q_z^+) = 0$$

where q_z^+ is mechanical loading term

The resulting stress resultants are defined as:

$$\{M_x \ \ M_y \ \ M_{xy} \ \ M_x^* \ \ M_y^* \ \ M_{xy}^*\} = \sum_{L=1}^{NL}\int_{Z_L}^{Z_{L+1}}\{\sigma_x z \ \ \sigma_y z \ \ \tau_{xy}z \ \ \sigma_x z^3 \ \ \sigma_y z^3 \ \ \tau_{xy}z^3\}dz,$$

$$\{Q_x \ \ Q_y \ \ Q_x^* \ \ Q_y^*\} = \sum_{L=1}^{NL}\int_{Z_L}^{Z_{L+1}}\{\tau_{xz} \ \ \tau_{yz} \ \ \tau_{xz}z^2 \ \ \tau_{yz}z^2\}dz,$$

$$\{S_x \ \ S_y \ \ S_x^* \ \ S_y^*\} = \sum_{L=1}^{NL}\int_{Z_L}^{Z_{L+1}}\{\tau_{xz}z \ \ \tau_{yz}z \ \ \tau_{xz}z^3 \ \ \tau_{yz}z^3\}dz,$$

$$\{N_x \ \ N_y \ \ N_{xy} \ \ N_z\} = \sum_{L=1}^{NL}\int_{Z_L}^{Z_{L+1}}\{\sigma_x \ \ \sigma_y \ \ \tau_{xz} \ \ \sigma_z\}dz,$$

$$\{N_x^* \ \ N_y^* \ \ N_{xy}^* \ \ N_z^*\} = \sum_{L=1}^{NL}\int_{Z_L}^{Z_{L+1}}\{\sigma_x z^2 \ \ \sigma_y z^2 \ \ \tau_{xy}z^2 \ \ \sigma_z z^2\}dz,$$

$$M_z = \sum_{L=1}^{NL}\int_{Z_L}^{Z_{L+1}}\{\sigma_z z\}dz. \tag{15}$$

Following are the mechanical boundary conditions used for simply supported plate.

At edges $x = 0$ and $x = a$:

$$v_0 = 0, w_0 = 0, \theta_y = 0, \theta_z = 0, M_x = 0, N_x = 0, v_0^* = 0, w_0^* = 0,$$
$$\theta_y^* = 0, \theta_z^* = 0,$$
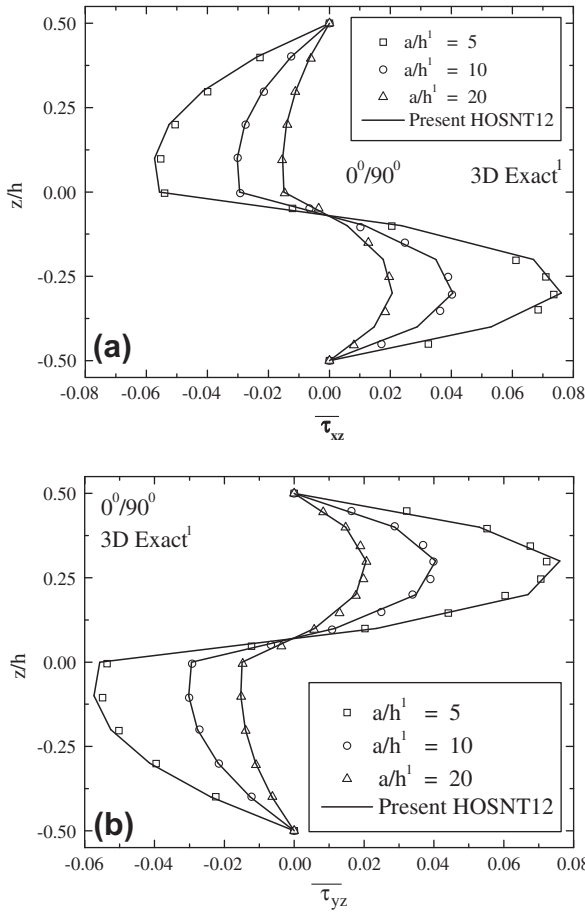
Fig. 4. Variation of normalized transverse shear stress (a) $\bar{\tau}_{xz}$, and (b) $\bar{\tau}_{yz}$ through the thickness of an unsymmetric [0°/90°] laminate under gradient thermal loading for a/h = 5, 10, and 20.

Fig. 5. Variation of normalized (a) inplane displacement $\bar{u}$, and (b) transverse displacement $\bar{w}$ through the thickness of a symmetric (0°/90°/0°) laminate under gradient thermal loading for a/h = 5, 10, and 20.

$M_x^* = 0, N_x^* = 0,$

At edges $y = 0$ and $y = b$:

$u_0 = 0, w_0 = 0, \theta_x = 0, \theta_z = 0, M_y = 0, N_y = 0, u_0^* = 0, w_0^* = 0, \theta_x^*$
$= 0, \theta_z^* = 0,$

$M_y^* = 0, N_y^* = 0,$

$$\{u_0 \quad \theta_x \quad u_0^* \quad \theta_x^*\} = \sum_{m=1,3,5}^{\infty} \sum_{n=1,3,5}^{\infty} \{u_{0_{mn}} \quad \theta_{x_{mn}} \quad u_{0_{mn}}^* \quad \theta_{x_{mn}}^*\} \cos\left(\frac{m\pi x}{a}\right) \sin\left(\frac{n\pi y}{b}\right)$$

$$\left\{v_0 \quad \theta_y \quad v_0^* \quad \theta_y^*\right\} = \sum_{m=1,3,5}^{\infty} \sum_{n=1,3,5}^{\infty} \left\{v_{0_{mn}} \quad \theta_{y_{mn}} \quad v_{0_{mn}}^* \quad \theta_{y_{mn}}^*\right\} \sin\left(\frac{m\pi x}{a}\right) \cos\left(\frac{n\pi y}{b}\right)$$

$$\{w_0 \quad \theta_z \quad w_0^* \quad \theta_z^*\} = \sum_{m=1,3,5}^{\infty} \sum_{n=1,3,5}^{\infty} \{w_{0_{mn}} \quad \theta_{z_{mn}} \quad w_{0_{mn}}^* \quad \theta_{z_{mn}}^*\} \sin\left(\frac{m\pi x}{a}\right) \sin\left(\frac{n\pi y}{b}\right)$$

$$\tag{16}$$

The thermal load is expressed as doubly sinusoidal loading at top of the laminate as.

$$T = \sum_{m=1,3,5}^{\infty} \sum_{n=1,3,5}^{\infty} T(z)_{mn} \sin\left(\frac{m\pi x}{a}\right) \sin\left(\frac{n\pi y}{b}\right) \tag{17}$$

$T(z)$ is obtained by considering equal rise and fall of the temperatures at top and bottom of the laminate surface as

$$T(x, y, \pm h/2) = \pm T_0 \sin\left(\frac{m\pi x}{a}\right) \sin\left(\frac{n\pi y}{b}\right) \tag{18}$$

To suit the above temperature gradient, linear thermal loading across the thickness is given by $T(z) = 2T_0 z/h$, where h is the total thickness of the laminate.

Transverse shearing stresses and normal stresses are calculated by integrating the equilibrium equations of elasticity, i.e.,

$$\tau_{xz} = -\sum_{L=1}^{n} \int_{z_{L-1}}^{z_L} \left(\frac{\partial \sigma_x}{\partial x} + \frac{\partial \tau_{xy}}{\partial y}\right) dz, \ \tau_{yz}$$

$$= -\sum_{L=1}^{n} \int_{z_{L-1}}^{z_L} \left(\frac{\partial \sigma_y}{\partial y} + \frac{\partial \tau_{xy}}{\partial x}\right) dz, \ \sigma_z$$

$$= -\sum_{L=1}^{n} \int_{z_{L-1}}^{z_L} \left(\frac{\partial \tau_{xz}}{\partial x} + \frac{\partial \tau_{yz}}{\partial y}\right) dz \tag{19}$$

3. Numerical results

Following configurations of the laminates are used for the thermal stress analysis under thermal gradient considering $m = 1$ and $n = 1$.

(a) Unsymmetrical laminated plate (0°/90°),
(b) Symmetric laminated plate (0°/90°/0°),
(c) Symmetric laminated plate (0°/90°/90°/0°) and
(d) Unsymmetrical laminated plate (90°/0°/90°/0°).

The lamina properties and the normalization coefficients for of numerical results are tabulated in Table 1.

Table 2
Normalized displacements $(\bar{u}, \bar{v}, \bar{w})$ and stresses $(\bar{\sigma}_x, \bar{\sigma}_y, \bar{\tau}_{xy}, \bar{\tau}_{xz}, \bar{\tau}_{yz})$ for three layered cross-ply (0°/90°/0°) laminated square plate simply supported on all edges subjected to gradient thermal loading.

a/h	SO	$\bar{u}$	$\bar{v}$	$\bar{w}$	$\bar{\sigma}_x$	$\bar{\sigma}_y$	$\bar{\tau}_{xy}$	$\bar{\tau}_{xz}$	$\bar{\tau}_{yz}$
2	PT	19.296 [−3.71]	143.408 [−5.27]	98.121 [1.37]	1334.96 [−3.95]	−654.37 [2.98]	−255.94 [−4.95]	52.531 [−17.81]	−205.25 [22.25]
	3D [12]	20.04	151.4	96.79	1390.00	−635.4	269.3	63.92	167.9
4	PT	18.178 [0.37]	75.9776 [−7.15]	42.020 [1.56]	1189.39 [0.54]	−871.19 [1.76]	−148.11 [−5.65]	88.618 [4.49]	−136.27 [5.88]
	3D [12]	18.11	81.83	42.69	1183.00	−856.1	−157.00	84.81	128.7
10	PT	16.531 [−0.47]	30.1846 [−3.71]	16.890 [−2.88]	1020.33 [−0.55]	−1019.28 [0.52]	−73.48 [−3.67]	61.715 [1.94]	−66.722 [1.07]
	3D [12]	16.61	31.35	17.39	1026.00	−1014.00	−76.29	60.54	−66.01
20	PT	16.128 [−0.26]	19.8194 [−2.55]	11.953 [1.37]	979.754 [−0.22]	−1052.76 [0.16]	−56.54 [−1.39]	34.174 [0.57]	−34.862 [0.29]
	3D [12]	16.17	20.34	12.12	982.00	−1051.00	−57.35	33.98	−34.76
50	PT	16.00 [−0.11]	16.6067 [−0.61]	10.468 [−0.36]	967.113 [−0.04]	−1063.14 [0.01]	−51.30 [−0.22]	14.08 [0.07]	−14.13 [0.00]
	3D [12]	16.02	16.71	10.50	967.5	1063.00	51.41	14.07	14.13
100	PT	15.983 [−0.10]	16.1352 [−0.103]	10.2442 [−0.15]	965.256 [−0.01]	−1065.00 [0.00]	−50.53 [0.00]	7.075 [0.02]	−7.080 [0.00]
	3D [12]	16.00	16.17	10.26	965.4	−1065.00	−50.53	7.073	−7.080

[12] 3D Exact, PT – present HOSNT12 [1], SO – Source, a/h – Aspect Ratio, [ ] % error = (present − exact) × 100/Exact.
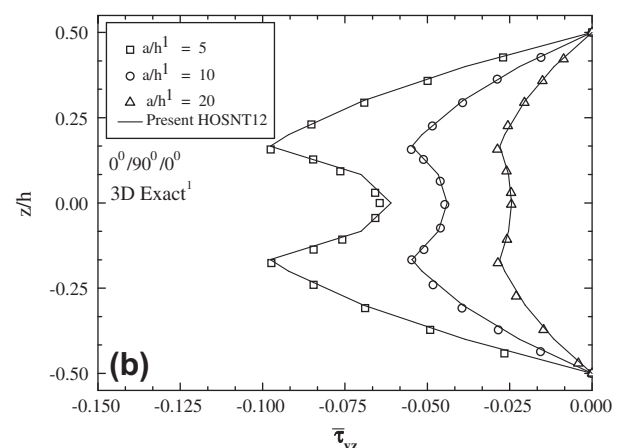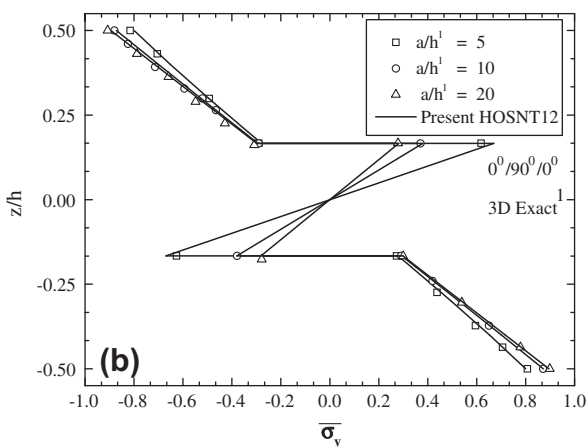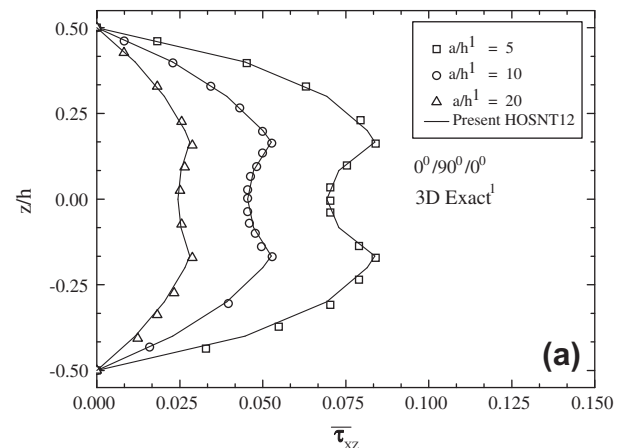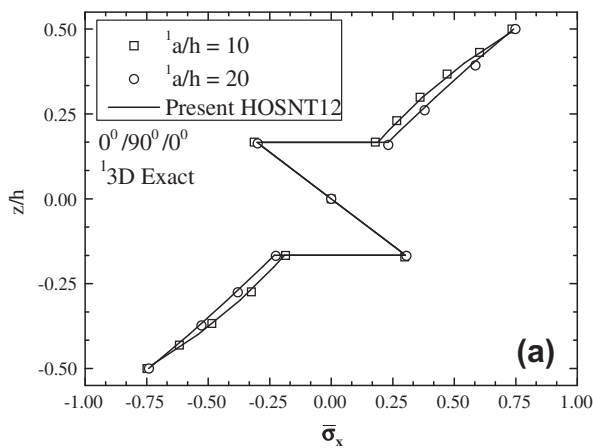
Fig. 6. Variation of normalized inplane normal stress (a) $\bar{\sigma}_x$ for a/h = 10, and 20, and (b) $\bar{\sigma}_y$ through the thickness of a symmetric (0°/90°/0°) laminate under gradient thermal loading for a/h = 5, 10, and 20.

Fig. 7. Variation of normalized transverse shear stress (a) $\bar{\tau}_{xz}$, and (b) $\bar{\tau}_{yz}$ through the thickness of a symmetric)0°/90°/0°) laminate under gradient thermal loading for a/h = 5, 10, and 20.

The results are compared with published results of exact solution, higher order zig-zag theory (HZIGT) and zig-zag theory (ZIGT) solutions in which transverse displacement is assumed constant through the thickness and thermal expansion coefficient in z direction is taken as zero and third order shear deformation theory,

(TOT) [13]. Matsunaga [16] computed 3D exact results following the formulations of Pagano [17] and also presented two-dimensional global higher-order shear deformation theory for multilayered laminates and sandwiches.

Table 3
Normalized displacements and stresses for square (b/a = 1) symmetric (0°/90°/90°/0°) laminate simply supported on all edges subjected to gradient thermal loading.

Quantity	a/h	Exact [12]	Present HOSNT12 [1]	HZIGT [13]	ZIGT [13]	TOT [13]
w (−0.5 h)	5	2.75290	2.79138 [1.40]	[−9.70]	[−38.03]	[−43.02]
	10	1.64490	1.64287 [−0.12]	[−4.01]	[−16.10]	[−19.56]
	20	1.31550	1.31398 [−0.12]	[−1.24]	[−5.04]	[−6.29]
	40	1.22830	1.22789 [−0.03]	[−0.33]	[−1.34]	[−1.69]
w (0.0 h)	5	1.51260	1.51064 [−0.13]	[0.29]	[12.79]	[3.70]
	10	1.32500	1.32039 [−0.35]	[0.45]	[4.16]	[−0.14]
	20	1.23490	1.23316 [−0.14]	[0.15]	[1.16]	[−0.18]
	40	1.20810	1.20768 [−0.03]	[0.05]	[0.31]	[−0.05]
σ_x (0.5 h)	5	0.74627	0.77721 [4.15]	[−2.74]	[−17.66]	[−34.78]
	10	0.75237	0.76048 [1.08]	[−1.02]	[−4.88]	[−10.38]
	20	0.76033	0.76241 [0.27]	[−0.28]	[−1.24]	[−2.71]
	40	0.76299	0.76351 [0.07]	[−0.07]	[−0.31]	[−0.68]
σ_y (−0.25 h)	5	−0.75104	−0.79404 [5.72]	[8.89]	[14.52]	[13.82]
	10	−0.51518	−0.52420 [1.75]	[3.76]	[6.12]	[4.57]
	20	−0.41917	−0.42115 [0.47]	[1.20]	[1.95]	[1.29]
	40	−0.39155	−0.39202 [0.12]	[0.32]	[0.53]	[0.33]
τ_{xy} (0.5 h)	5	−0.13164	−0.13120 [−0.34]	[−7.54]	[−14.68]	[−18.14]
	10	−0.09746	−0.09696 [−0.52]	[−2.34]	[−4.71]	[−6.72]
	20	−0.08682	−0.08623 [−0.68	[−0.63]	[−1.30]	[−1.96]
	40	−0.08339	−0.08334 [−0.06	[−0.16]	[−0.33]	[−0.51]
τ_{xz} (0.0 h)	5	0.19328	0.19410 [0.42]	[−5.71]	[−4.78]	[5.38]
	10	0.28502	0.28661 [0.56]	[−1.22]	[−1.20]	[1.76]
	20	0.31933	0.31988 [0.17]	[−0.29]	[−0.29]	[0.48]
	40	0.32901	0.32916 [0.04]	[−0.07]	[−0.07]	[0.12]
τ_{yz} (0.0 h)	5	−0.14025	−0.13323 [−5.01]	[−30.78]	[−47.82]	[−40.45]
	10	−0.26317	−0.26309 [−0.03]	[−4.60]	[−7.20]	[−4.71]
	20	−0.31303	−0.31323 [0.06]	[−0.99]	[−1.56]	[−0.89]
	40	−0.32737	−0.32744 [0.02]	[−0.24]	[−0.38]	[−0.20]

[12] 3D-Exact, present HOSNT12 [1] – {higher order zig-zag theory (HZIGT), zig-zag theory (ZIGT), third order theory (TOT)}, [ ] % error = (present − exact) × 100/exact.

Table 4
Normalized displacements and stresses for rectangular (b/a = 2) symmetric (0°/90°/90°/0°) laminated plate subjected to gradient thermal loading.

Quantity	a/h	Exact [12]	Present HOSNT12 [1]	HZIGT [13]	ZIGT [13]	TOT [13]
w (−0.5 h)	5	1.99510	2.03454 [1.98]	[−12.67]	[−50.44]	[−51.20]
	10	1.07800	1.08250 [0.42]	[−5.96]	[−23.94]	[−24.60]
	20	0.83326	0.83400 [0.09]	[−1.94]	[−7.79]	[−8.04]
	40	0.77097	0.77113 [0.02]	[−0.52]	[−2.11]	[−2.18]
w (0.0 h)	5	0.71047	0.72012 [1.36]	[7.57]	[39.16]	[37.04]
	10	0.75036	0.75296 [0.35]	[1.97]	[9.28]	[8.32]
	20	0.75093	0.75155 [0.08]	[0.50]	[2.32]	[2.04]
	40	0.75036	0.75051 [0.02]	[0.13]	[0.58]	[0.51]
σ_x (−0.5 h)	5	−0.46412	−0.47833 [3.06]	[−2.53]	[−23.45]	[−34.55]
	10	−0.38786	−0.39111 [0.84]	[−1.04]	[−7.50]	[−11.32]
	20	−0.36644	−0.36726 [0.22]	[−0.30]	[−2.02]	[−3.07]
	40	−0.36091	−0.36116 [0.07]	[−0.08]	[−0.52]	[−0.78]
σ_y (−0.5 h)	5	0.96525	0.96428 [−0.10]	[0.23]	[0.53]	[0.36]
	10	0.97960	0.97937 [−0.02]	[0.06]	[0.13]	[0.09]
	20	0.98363	0.98354 [−0.01]	[0.01]	[0.03]	[0.02]
	40	0.98467	0.98462 [−0.01]	[0.00]	[0.01]	[0.01]
τ_{xy} (−0.5 h)	5	0.05294	0.05247 [−0.88]	[−5.78]	[−12.91]	[−8.34
	10	0.03323	0.03298 [−0.75]	[−2.31]	[−5.26]	[−3.33]
	20	0.02768	0.02761 [−0.26]	[−0.69]	[−1.59]	[−1.00]
	40	0.02625	0.02623 [−0.08]	[−0.18]	[−0.42]	[−0.26]
τ_{xz} (0.0 h)	5	0.01013	0.00674 [−33.46]	[−16.66]	[51.43]	[88.39]
	10	0.02589	0.02518 [−2.75]	[−1.29]	[5.67]	[9.94]
	20	0.03053	0.03034 [−0.62]	[−0.25]	[1.24]	[2.19]
	40	0.03175	0.03167 [−0.26]	[−0.06]	[0.30]	[0.53]
τ_{yz} (0.0 h)	5	−0.23707	−0.24150 [1.87]	[−2.07]	[−4.37]	[−5.80]
	10	−0.26932	−0.27066 [0.50]	[−0.48]	[−0.99]	[−1.32]
	20	−0.27871	−0.27907 [0.13]	[−0.12]	[−0.24]	[−0.32]
	40	−0.28115	−0.28126 [0.04]	[−0.03]	[−0.06]	[−0.08]

[ ] % Error = (present − exact) × 100/exact.

Table 5
Normalized displacements and stresses for square unsymmetric (90°/0°/90°/0°) laminated plate subjected to gradient thermal loading.

Quantity	a/h	Exact [12]	Present HOSNT12 [1]	HZIGT [13]	ZIGT [13]	TOT [13]
w (−0.5 h)	5	2.78690	2.72833 [−2.10]	[−11.53]	[−39.57]	[−47.18]
	10	1.84550	1.81823 [−1.48]	[−4.90]	[−15.82]	[−18.79]
	20	1.59370	1.58640 [−0.46]	[−1.47]	[−4.65]	[−5.52]
	40	1.52960	1.52816 [−0.09]	[−0.39]	[−1.22]	[−1.44]
w (0.0 h)	5	1.54920	1.45080 [−6.35]	[−3.38]	[8.71]	[−4.98]
	10	1.52760	1.49774 [−1.95]	[−1.35]	[1.70]	[−1.89]
	20	1.51360	1.50621 [−0.49]	[−0.38]	[0.40]	[−0.52]
	40	1.50950	1.50811 [−0.09]	[−0.09]	[0.10]	[−0.13]
σ_x (0.5 h)	5	0.64727	0.64434 [−0.45]	[5.21]	[−11.00]	[−15.49]
	10	0.59169	0.58960 [−0.35]	[1.23]	[-3.34]	[−4.61]
	20	0.57588	0.57529 [−0.10]	[0.30]	[−0.88]	[−1.21]
	40	0.57180	0.57167 [−0.02]	[0.08]	[-0.22]	[−0.31]
σ_y (0.5 h)	5	−0.84264	−0.84209 [−0.07]	[4.22]	[5.38]	[5.88]
	10	−0.87679	−0.87744 [0.07]	[1.13]	[1.41]	[1.54]
	20	−0.88632	−0.88678 [0.05]	[0.29]	[0.36]	[0.39]
	40	−0.88877	−0.88915 [0.04]	[0.07]	[0.09]	[0.10]
τ_{xy} (0.5 h)	5	−0.13797	−0.13587 [−1.52]	[−16.98]	[−24.00]	[−26.69]
	10	−0.11299	−0.11205 [−0.83]	[−5.80]	[−8.01]	[−8.86]
	20	−0.10601	−0.10578 [−0.22]	[−1.59]	[−2.19]	[−2.41]
	40	−0.10422	−0.10419 [−0.03]	[−0.41]	[−0.57]	[−0.62]
τ_{xz} (0.25 h)	5	0.26478	0.28572 [7.91]	[8.79]	[10.16]	[11.75]
	10	0.29420	0.30015 [2.02]	[2.25]	[2.58]	[2.95]
	20	0.30246	0.30396 [0.50]	[0.57]	[0.65]	[0.74]
	40	0.30459	0.30493 [0.11]	[0.14]	[0.16]	[0.18]
τ_{yz} (0.25 h)	5	−0.41447	−0.43692 [5.42]	[7.09]	[7.63]	[8.13]
	10	−0.44710	−0.45353 [1.44]	[1.82]	[1.95]	[2.06]
	20	−0.45608	−0.45793 [0.41]	[0.46]	[0.49]	[0.52]
	40	−0.45839	−0.45904 [0.14]	[0.11]	[0.12]	[0.13]

[ ] % Error = (present − exact) × 100/exact.

Example 1. A simply supported square unsymmetric (0°/90°) laminate under bi-directional bending subjected to gradient thermal loading is analyzed and results are compared with 3D elasticity solution [16]. Fig. 2 shows variation of normalized transverse displacement ($\bar{w}$) and in-plane displacement ($\bar{u}$) across the thickness of the laminate. It is clear from the graph that the transverse displacement ($\bar{w}$) is constant and in-plane displacement ($\bar{u}$) is linear over the thickness. Cubical variation in primary displacement field is quite sufficient to express the displacements. Fig. 3 presents the variations in in-plane normal stresses ($\bar{\sigma}_x, \bar{\sigma}_y$) across the thickness. Present theory, HOST 12 [1] underestimates the values at extreme faces of the thick laminates (a/h = 5). Fig. 4 demonstrates variations in transverse shear stresses ($\bar{\tau}_{xz}, \bar{\tau}_{yz}$) where the results of the present theory are seen to be to that of the exact solutions for thin (a/h = 20) as well as thick (a/h = 5) laminates. The transverse shear and normal stresses ($\bar{\tau}_{xz}, \bar{\tau}_{yz}, \bar{\sigma}_z$) are evaluated through integration of equilibrium equations of elasticity.

Example 2. A simply supported square cross-ply symmetric (0°/90°/0°) laminated plate under bi-directional bending and subjected to linear thermal profile is presented here. Normalized results for in-plane displacements ($\bar{u}$), transverse displacements ($\bar{w}$), in-plane normal stresses ($\bar{\sigma}_x, \bar{\sigma}_y$) and in-plane shear ($\bar{\tau}_{xy}$), transverse shear stresses ($\bar{\tau}_{xz}, \bar{\tau}_{yz}$) are tabulated in Table 2. Results are compared with 3D elasticity solution [12] for very thick (a/h = 2) to thin (a/h = 100) laminates and the present results are in good agreement with elasticity solution.

Variations of the quantities over the thickness of the laminates are expressed in the figures and compared with the 3D elasticity solutions published [16]. Fig. 5a and b shows variations of in-plane displacements ($\bar{u}$) and transverse displacements ($\bar{w}$) respectively for aspect ratios 5, 10 and 20. Non-linear variations are observed in the displacement quantities especially for a thick laminate (a/h = 5). Variations in in-plane stresses ($\bar{\sigma}_x, \bar{\sigma}_y$) for various aspect ratios are displayed in Fig. 6 and transverse shear stresses ($\bar{\tau}_{xz}, \bar{\tau}_{yz}$) are demonstrated in Fig. 7.

Example 3. A simply supported square (b/a = 1) symmetric (0°/90°/90°/0°) laminated plate under bi-directional bending and subjected to linear thermal profile is discussed here. Numerical results are tabulated in Table 3. Results of present HOST 12 [1] for transverse displacement ($\bar{w}$) are more accurate than other models. Present HOST12 [1], overestimates the values of the results for in-plane normal stresses ($\bar{\sigma}_x, \bar{\sigma}_y$) by 4–5% for thick (a/h = 5) laminate. In case of in-plane shear stress ($\bar{\tau}_{xy}$), present HOST12 [1] provides very accurate values compared to other models. ZIGT provides large errors in the stress quantities. Results of transverse shear stresses ($\bar{\tau}_{xz}$) are excellent as compared with HZIGT, where % errors in ($\bar{\tau}_{xz}$) are same for HZIGT and ZIGT. Underestimation of transverse shear stresses ($\bar{\tau}_{yz}$) is observed in case of present HOST12 [1], by about 5%, where as other theories provide very large errors up to 47%.

Example 4. A simply supported rectangular (b/a = 2) symmetric (0°/90°/90°/0°) laminated plate under bi-directional bending and subjected to linear thermal profile is considered. Numerical results are compared in Table 4. Results of present theory for transverse displacement ($\bar{w}$) show excellent agreement with exact results as compare to other models [13]. The % error in present HOST12 [1], for in-plane stresses ($\bar{\sigma}_x$) is marginally more than HZIGT model but for in-plane stress ($\bar{\sigma}_y$), results are excellent. The % error in present HOST12 [1], model for transverse shear stresses ($\bar{\tau}_{xz}$) is more than HZIGT results for all aspect ratios. Present results for in-plane shear stress ($\bar{\tau}_{xy}$) and transverse shear stress ($\bar{\tau}_{yz}$) are close to exact solution.
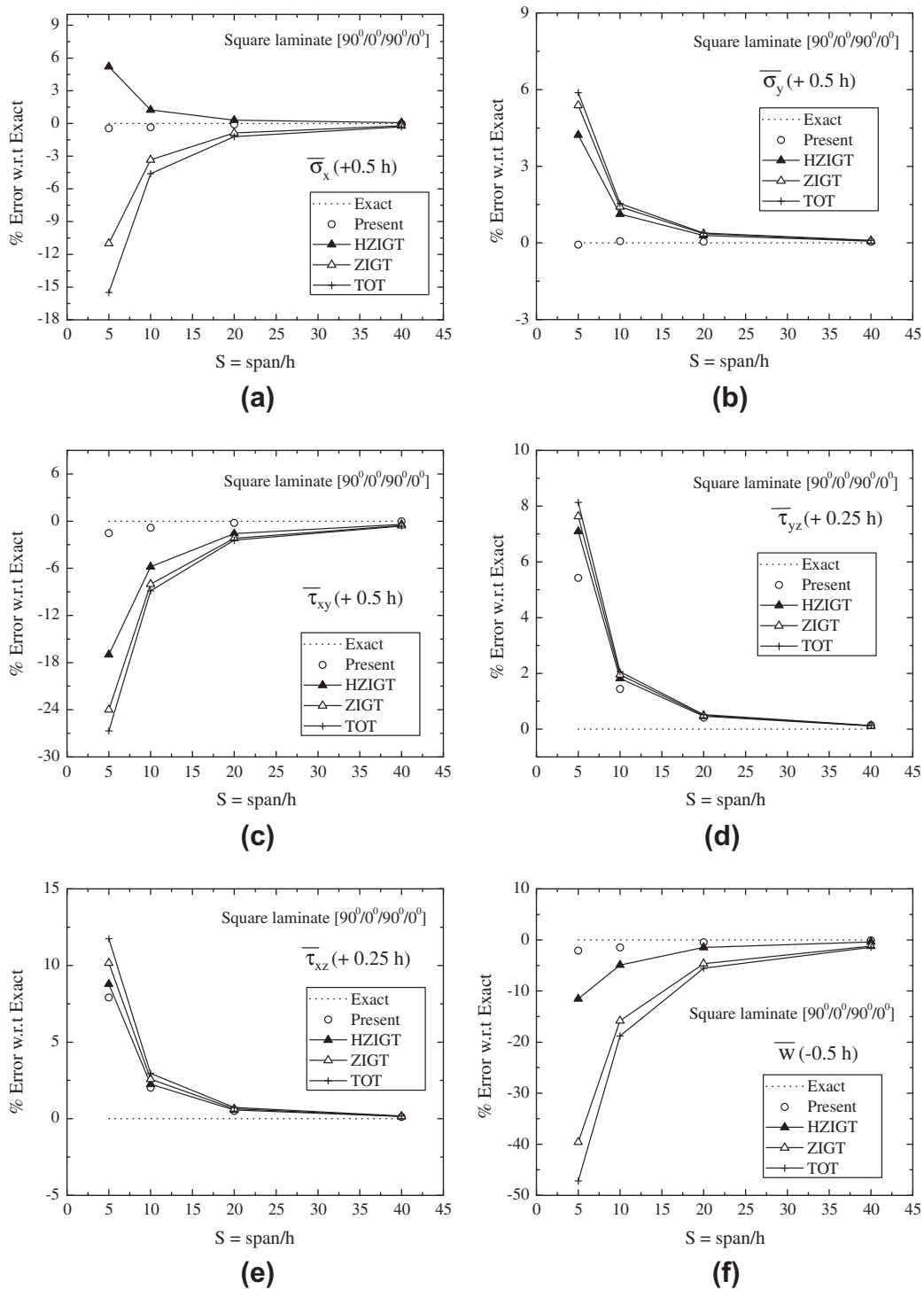
Fig. 8. Variations of % errors with respect to span to thickness ratios (S = span/h) of square laminate (90°/0°/90°/0°) of various theories.

Example 5. A simply supported square (b/a = 1) unsymmetric (90°/0°/90°/0°) laminated plate under bi-directional bending and subjected to thermal gradient is presented here. Numerical results are compared in Table 5. The present numerical results for transverse displacement ($\bar{w}$), at top of the laminate are close to exact solution but mid-plane results are deviating by more than 6%. Excellent results are observed for in-plane normal stresses as well as in-plane shear stresses ($\bar{\sigma}_x$, $\bar{\sigma}_y$, $\bar{\tau}_{xy}$). The present results are deviating by more than 7% for transverse shear stresses ($\bar{\tau}_{xz}$, $\bar{\tau}_{yz}$) in case of thick laminates (a/h = 5). Graphical variations of % errors

with respect to aspect ratios for various theories are demonstrated in Fig. 8.

4. Conclusions

An efficient higher order shear and normal deformation theory with twelve degrees of freedom in primary displacement field HOSNT12 [1] is presented for thermal stress analysis of composite laminates. Present theory accounts for thermal expansion coeffi-

cient in the transverse normal direction in addition to planner directions. Thermal loading with doubly sinusoidal variation along *x* and *y* directions and linear or gradient thermal fields along thickness direction is considered over the cross-ply laminates. The present HOSNT12 [1] is assessed by comparison with the 3D exact and other 2D models. ZIGT and TOT provide good results only in case of very thin laminates with aspect ratio (a/h) of more than 40. HZIGT estimates fairly accurate results for the moderately thick (a/h = 10) to thin plate (a/h > 10).

It is clear from the comparisons, that the performance of present HOSNT12 [1] model (which also accounts for thermal strains in transverse normal direction) is excellent in the estimation of global as well as local quantities of laminates subjected to thermal gradient for almost all aspect ratios.

References

[1] Kant T, Swaminathan K. Analytical solutions for static analysis of laminated composite and sandwich plates based on a higher order refined theory. Compos Struct 2002;56:329–44.

[2] Timoshenko SP, Woinowsky-Krieger S. Theory of plates and shells. McGraw-Hill; 1959.

[3] Reissner E. The effect of transverse shear deformation on the bending of elastic plates. ASME J Appl Mech 1945;12:69–77.

[4] Mindlin RD. Influence of rotatory inertia and shear deformation on flexural motions of isotropic elastic plates. ASME J Appl Mech 1951;18:31–8.

[5] Reddy JN, Chao WC. Finite element analysis of laminated bimodulus composite material plates. Comput Struct 1980;12:245–51.

[6] Argyris JH, Tenek L. High temperature bending, buckling and postbuckling of laminated composite plates using the natural mode method. Comput Methods Appl Mech Eng 1994;117:105–42.

[7] Khdeir AA, Reddy JN. Thermal stresses and deflections of cross ply laminated plates using refined plate theories. J Therm Stresses 1991;14:419–39.

[8] Kant T, Khare RK. Finite element thermal stress analysis of composite laminates using a higher-order theory. J Therm Stresses 1994;17:229–55.

[9] Rohwer K, Rolfes R, Sparr. Higher-order theories for thermal stresses in layered plates. Int J Solids Struct 2001;38:3673–87.

[10] Tungikar VB, Rao KM. Three-dimensional exact solution of thermal stresses in rectangular composite laminate. Compos Struct 1994;27:419–30.

[11] Savoia M, Reddy JN. Three-dimensional thermal analysis of laminated composite plates. Int J Solids Struct 1995;32:593–608.

[12] Bhaskar K, Varadan TK, Ali JSM. Thermoelastic solutions for orthotropic and anisotropic composite laminates. Composites: Part B 1996;27B:415–20.

[13] Kapuria S, Achary GGS. An efficient higher order zigzag theory for laminated plates subjected to thermal loading. Int J Solids Struct 2004;41(16–17):4661–84.

[14] Kant T, Desai Y, Pendhari S. An efficient semi-analytical model for composite and sandwich plate subjected to thermal load. J Therm Stresses 2008;31:77–103.

[15] Tauchart TR. Stresses in plates – statical problems. In: Hetnarski RB, editor. Thermal Stresses I. New York: Elsevier; 1986.

[16] Matsunaga H. A comparison between 2-D single-layer and 3-D layerwise theories for computing interlaminar stresses of laminated composite and sandwich plates subjected to thermal loadings. Compos Struct 2004;64:161–77.

[17] Pagano NJ. Exact solution for composite laminated in cylindrical bending. J Compos Mater 1969;3:398–411.